Bioorganic & Medicinal Chemistry xxx (2013) xxx–xxx

Contents lists available at ScienceDirect

Bioorganic & Medicinal Chemistry

journal homepage: www.elsevier.com/locate/bmc

Design, synthesis, and enzyme kinetics of novel benzimidazole and quinoxaline derivatives as methionine synthase inhibitors

Hosam Elshihawy [a], Mohamed A. Helal [b], Mohamed Said [a], Mohamed A. Hammad [c,*]

[a] Organic Chemistry Department, Faculty of Pharmacy, Suez Canal University, Ismailia 41522, Egypt
[b] Pharmaceutical Chemistry Department, Faculty of Pharmacy, Suez Canal University, Ismailia 41522, Egypt
[c] Eli & Edythe Broad CIRM Center for Regenerative Medicine and Stem Cell Research, Keck School of Medicine, University of Southern California, 1425 San Pablo Street, BCC 505, Los Angeles, CA 90033, USA

ARTICLE INFO

Article history:
Received 4 September 2013
Revised 19 October 2013
Accepted 29 October 2013
Available online xxxx

Keywords:
Benzimidazole
Quinoxaline
Methionine synthase
5-Methyltetrahydrofolate
Cancer

ABSTRACT

Methionine synthase catalyzes the transfer of a methyl group from 5-methyltetrahydrofolate to homocysteine, producing methionine and tetrahydrofolate. Benzimidazole and deazatetrahydrofolates derivatives have been shown to inhibit methionine synthase by competing with the substrate 5-methyltetrahydrofolate. In this study, a novel series of substituted benzimidazoles and quinoxalines were designed and assessed for inhibitory activity against purified rat liver methionine synthase using a radiometric enzyme assay. Compounds **3g**, **3j**, and **5c** showed the highest activity against methionine synthase (IC_{50}: 20 μM, 18 μM, 9 μM, respectively). Kinetic analysis of these compounds using Lineweaver–Burk plots revealed characteristics of mixed inhibition for **3g** and **5c**; and uncompetitive inhibition for **3j**. Docking study into a homology model of the rat methionine synthase gave insights into the molecular determinants of the activity of this class of compounds. The identification of these drug-like inhibitors could lead the design of the next generation modulators of methionine synthase.

1. Introduction

Cobalamin-dependant methionine synthase (MetS) (EC.2.1.1.13) is one of the transmethylase enzymes that utilizes cobalamin derivative methylcobalamin (Me-Cbl) as a cofactor.[1] This enzyme plays a crucial role in folate cycle and methionine (Met) metabolism. MetS catalyzes the transfer of the methyl group from 5-methyltetrahydrofolate (MeTHF) to homocysteine (Hcy) via the cobalamin cofactor (Cbl) which circulates between +1 and +3 oxidation states.[2,3] The enzyme functions in two steps as a ping-pong mechanism. First, it transfers methyl group from MeTHF to enzyme-bound cobalamin (Cbl(I)) to generate methyl-cobalamin(III) (Me-Cbl(III)) and tetrahydrofolate. Second, the methyl group is transferred from the generated Me-Cbl(III) to Hcy producing Met with the regeneration of Cbl(I) (Fig. 1). Cobalamin-dependent methionine synthase is found in mammalian tissues and microorganisms, while the plant enzyme is cobalamin-independent.[4] Crystal structure of cobalamin-dependent MetS revealed that it consists of four functional domains, namely, Hcy binding domain, MeTHF binding domain, cobalamin cofactor binding domain, and the allosteric cofactor *S*-adenosyl-methionine (*S*-AdoMet) binding domain.[5,6] The reaction products, tetrahydrofolate and Met are further metabolized via folate cycle and the one-carbon methionine transmethylation. It is worth noting that MetS is the only human enzyme that metabolizes MeTHF to regenerate the active form tetrahydrofolate. Therefore, it is essential in the recycling of different biological forms of folates required for purine and pyrimidine synthesis.[7] In the methionine transmethylation cycle, Met is transformed to the reactive *s*-adenosyl methionine (AdoMet) which is a biologically iumportant methyl donor involved in the synthesis of nucleic acids, epinephrine, and creatine. The product of this methylation process is *s*-adenosyl homocysteine which is readily hydrolysed to adenosine and homocysteine. The latter is again methylated to methionine using MetS enzyme; hence conserving the limited dietary supply of this essential amino acid.[8] Normal cells remain unaffected by Met restrictions if supplemented with Hcy, as they are able to synthesize Met via methylation of Hcy in sufficient quantities. Impaired function of MetS could lead to megaloblastic anaemias and neurological disorders.[9] From a medicinal chemistry point of view, inhibition of MetS would compromise DNA and RNA synthesis and provide a valuable tool for chemotherapeutic intervention in some cancers.[10,11]

Despite being an attractive target for rational drug design, MetS is not yet exploited to produce clinically useful anticancer agents. A number of studies have shown that frequent administration of ethanol resulted in the inhibition of methionine synthase via the interference with the conversion of hydroxycobalamin to methylcobalamin.[12] It was also reported that nitrous oxide (N_2O) inhibits

* Corresponding author. Tel.: +1 323 442 1688; fax: +1 323 442 8067.
E-mail address: mhammad@usc.edu (M.A. Hammad).

0968-0896/$ - see front matter © 2013 Elsevier Ltd. All rights reserved.
http://dx.doi.org/10.1016/j.bmc.2013.10.052

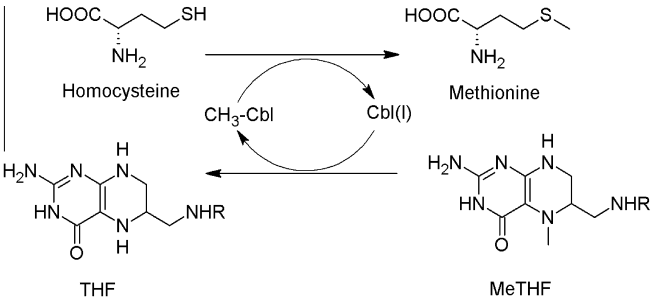

Figure 1. The cobalamin-dependent methionine synthase catalyzed methyl group transfer. Cbl(I): Cob(I)alamin, CH_3-Cbl: methylcob(III)alamin, MeTHF: methyl tetrahydrofolate.

the enzyme through oxidation of the cobalamin cofactor.[13] Other non-drug like inhibitors includes methylmercury, acetaldehyde, and some cobalamin analogs.[14,15] Therefore, we think that the design of drug-like small molecules as inhibitors of MetS has been overlooked. In a recent study, Zhang et al. reported some N_5-substituted 8-deazatetrahydrofolates as folate analogs inhibiting the enzyme by the formation of covalent bonds with the nucleophilic Cbl(I) cofactor. These inhibitors had shown some in vitro inhibitory activity against HL-60 cells.[16] In 2006, Banks et al. designed simple benzimidazole and benzothiadiazole derivatives and tested them in a cell free system for rat liver MetS inhibitory activity.[17] Despite being suitable drug leads, these compounds possessed limited diversity and only weak inhibitory activity against the enzyme with IC_{50} values around 100 μM.

In the present study, we decided to explore the utility of this benzimidazole scaffold to design MetS inhibitors that could compete with MeTHF for its binding pocket. Benzimidazole and quinoxaline derivatives that resemble the chemical substructure of MeTHF were designed by introducing alkyl and aryl side chains on the nitrogen containing ring. The heterocyclic nucleus should occupy the same pteridine-binding pocket while the diverse substituents could make contacts with other residues in the MeTHF domain, originally binding PABA and glutamate part, to enhance the activity and selectivity.

2. Results and discussion

2.1. Compounds design

Although the biochemical role of MetS in folate metabolism and nucleotide biosynthesis is well established, no clinically useful anticancer agents targeting this enzyme are available to date. As mentioned above, there are also a limited number of drug-like MetS inhibitors reported so far. We noticed that the weak benzimidazole and benzothiadiazole inhibitors designed by Banks et al. possess a relatively small size compared to the large binding site of MeTHF.[17] These compounds were designed to mimic the planar pteridine substructure of MeTHF and form polar contacts with Asn458, Asp525, and Asn567 in the pteridine binding pocket. On the other hand, the pocket created by Asn323, Arg516, and Phe570, originally binding PABA, remains vacant. In order to enhance the activity and the drug-like properties of this series of compounds, we envisioned a strategy in which acyl- and arylamino side chains are introduced at carbon 2 of the benzimidazole nucleus to occupy the PABA binding pocket and confer more binding ability on the compounds. In addition, we decided to prepare a series of quinoxaline derivatives to exploit their similar size and electronic characters to the pteridine nucleus of MeTHF. Also, Banks et al. showed that the presence of free NH and 5-nitro group on the benzimidazole ring is associated with stronger activity. Therefore, we decided to keep these features fixed and introduce diversity at position 2 of the benzimidazole or quinoxaline rings.

2.2. Chemistry

Phillips procedure was adapted for the synthesis of benzimidazole derivatives via a condensation reaction of o-phenylendiamines **1a**–**b** and the appropriate amino acids in the presence of 5.5 N HCl.[18] Then, acetylation or benzoylatoion of the obtained amines **2a**–**d** was affected using acetic anhydruide or benzoyl chloride, respectively. This method has furnished benzimidazole derivatives **3a**–**j** in moderate yields (Scheme 1). Quinoxalines **5a**–**d** have been synthesized through a condensation reaction between the appropriate aromatic aldehydes and 4-nitro-*o*-phenylendiamine (**1b**) according to the reported procedure.[19] The arylidene derivatives produced (**4a**–**d**) have been refluxed with triethyl orthoformate to give the required quinoxalines **5a**–**d**.[20] Finally, the target quinoxalines **6a**–**b** were obtained via the alkylation of **5b** with the appropriate alkyl halides, whilst the target compounds **7a**–**b** were obtained through the coupling of **5c** with the appropriate aliphatic amines under the standard amide coupling conditions (Scheme 2).

2.3. Biological evaluation

The target compounds that were successfully synthesized were tested for their inhibitory activity against highly purified rat liver cobalamin-dependent methionine synthase (Table 1). Generally, benzimidazoles with aliphatic side chains on carbon 2 showed significantly lower activities compared to those with aromatic ones (compare **3c** and **3g**). This could be attributed to the ability of the bulkier aryl substituents to make favorable contacts with the PABA binding pocket of MetS. We also noticed that the terminal aryl ring should be isolated from the benzimidazole nucleus with a polar three- to four-atom linker. Another feature that was found to greatly enhance the inhibitory activity was the presence of nitro group on carbon 5 of the benzimidazole ring (compare **3e** and **3g**). This nitro group is the bioisoster of the amino group at carbon atom 2 of the MeTHF pteridine ring. Phenylquinoxaline **5a** and its amino derivatives, **5b**, **6a**, and **6b** showed only moderate activity, whilst substitution of the phenyl ring with a carboxylic acid group increased the activity and gave the most active compound in this study (compound **5c**, IC_{50} = 9 μM). Further substitution on the terminal carboxylic acid groups could not improve the inhibitory activity (compounds **7a**–**b**). The most active compound, **5c**, Scheme 1 possesses a similar shape to the natural ligand, tetrahydrofolate. In addition, it has less polar functional groups and more rigid scaffold. Hence, it loses less entropy upon binding to the enzyme than tetrahydrofolate.

Methionine synthase is a bisubstrate enzyme binding both MeTFH as well as hmocysteine. It is possible that MetS inhibitors also compete for the homocysteine binding domain in addition to the MeTHF binding domain, or even bind at the site of the *S*-adenosyl methionine reactivation cofactor.[17] Therefore, the molecular mechanism of action of the most active compounds **5c**, **3g**, and **3j** was further investigated by studying the kinetic parameters of inhibition. These compounds were tested at gradient concentrations of 500 μM, 250 μM, 100 μM and 0 μM in a radiometric enzyme assay.[21] In this study we have only attempted the evaluation of the inhibitory activity against the MeTHF binding site, keeping all other parameters constant. The kinetic parameters of the enzyme inhibition were calculated and the Lineweaver-Burk plots were established for the inhibited reactions as well as the uninhibited reaction (K_m = 28.6 μM, V_{max} = 8.7 μM min^{-1}) (Fig. 2 and S4).[22] The Lineweaver–Burk plots for the inhibited reactions showed that compounds **5c** and **3g** exhibits the characteristics of mixed inhibition

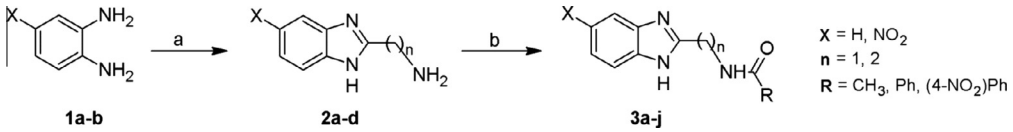

Scheme 1. Reagents and conditions: (a) L-amino acid, 5.5 M HCl, reflux, 5 h; (b) RCOCl, TEA, THF, reflux, 3 h.

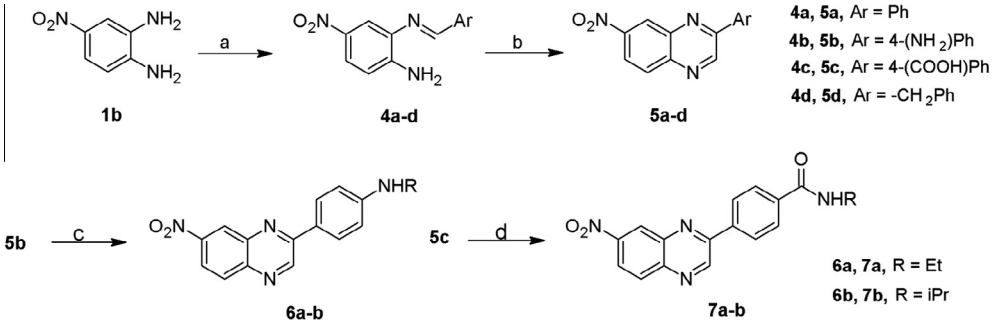

Scheme 2. Reagents and conditions: (a) ArCHO, EtOH, reflux, 12 h; (b) triethyl orthoformate, DMF, reflux, 24 h; (c) RBr, TEA, THF, reflux 24 h; (d) RCOOH, EDCI, HOBt, TEA, DCM, rt, 12 h.

Table 1
Chemical structures and IC_{50} of the prepared benzimidazoles

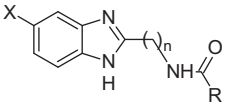

Compound	X	*n*	R	IC_{50} (μM)
3a	H	1	CH_3	NA[a]
3b	H	2	CH_3	NA
3c	NO_2	1	CH_3	NA
3d	NO_2	2	CH_3	NA
3e	H	1	Ph	122
3f	H	2	Ph	85
3g	NO_2	1	Ph	20
3h	NO_2	2	Ph	66
3i	H	1	4-(NO_2)Ph	73
3j	NO_2	2	4-(NO_2)Ph	18

Values were determined using highly purified rat liver methionine synthase.
[a] NA: not active.

which is a pattern typically noticed in multisubstrate enzymes such as MetS, whilst compound **3j** shows the behavior of uncompetitive inhibition. This uncompetitive inhibition indicates that there is no direct interaction between the inhibitor and the MeTHF binding site. Potential explanation includes the possibility that the inhibitor may bind at other binding sites such as the binding site of the MetS allosteric cofactor (*S*-AdoMet) or to the surface of whole enzyme. Also, due to the structure similarity, this nitrobenzimidazole **3j** may displace the dimethylbenzimidazole side chain of the cobalamin-cofactor. The molecular determinants of the uncompetitive inhibition of MetS will be the subject of future investigation in our laboratory.

2.4. Homology modeling and docking studies

To examine the mode of binding of the designed inhibitors to MetS and to investigate further their mechanism of action, compounds **5c**, **3g**, and **3j** were docked into the proposed MeTHF binding site in MetS. In the absence of a high-resolution crystal structure of the mammalian enzyme, a model of the rat MetS Hcy- and pterin-binding domains (residues: 1–620) was constructed, based on the X-ray crystal structure of MetS from *Thermotoga maritima* (PDB: 1Q8J).[6] It has been reported that the MeTHF binding domains of methyltransferases possess similar architecture.[23] The crystal structure of MetS from *T. maritime* showed that four polar residues, Asn411, Asp473, Asn508, and Arg516, are critical for the interaction with the substrate MeTHF. Our final refined model of rat MetS showed similar arrangement of the corresponding polar residues within the binding site of MeTHF, namely, Asn404, Asn458, Asp525, Asn567, and Arg579 (Fig. S3). Hence, the developed model should be able to rationalize the binding of the designed pterin isosteres into MetS.

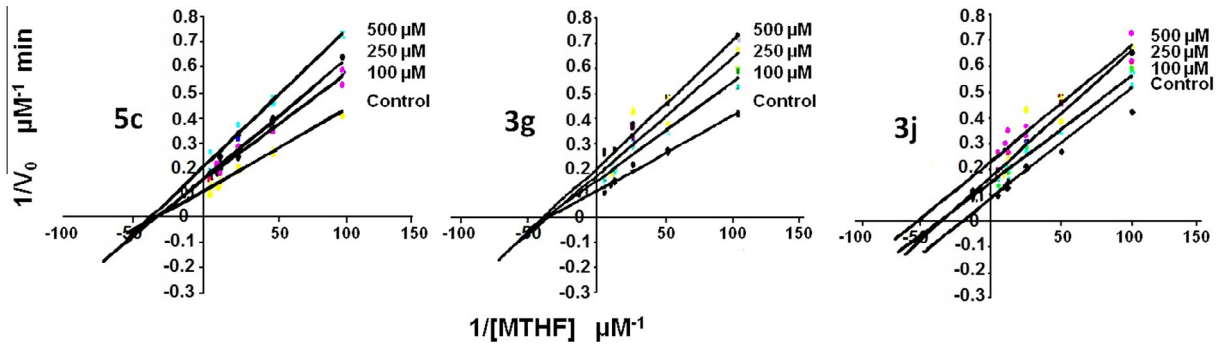

Figure 2. Lineweaver–Burk plots for compounds **5c**, **3g**, and **3j**, with respect to methyltetrahydrofolate (MeTHF), at inhibitor concentrations of 500 μM, 250 μM, 100 μM, and 0 μM.

Compounds **5c**, **3g**, and **3j** were docked into the MeTHF binding site, defined by a sphere of 10 Å radius around the side chain nitrogen of Asn458, using CCDC Gold software. As expected, compound **5c** showed more favorable interactions than **3g** or **3j**, taking into consideration that **3j** is an uncompetitive inhibitor. The docked conformation of **5c** shared a very similar binding mode to MeTHF in the template crystal structure (PDB ID: 1Q8J) with the quinoxaline nucleus having the same position as the pterin ring of MeTHF. Table 2 The nitro group, acting as a bioisotere of the pterin ring amino group, forms a strong H bond with Ser461. On the other side of the binding pocket, the carboxylic group shows another H bond with Arg579 similar to that formed by the PABA fragment of MeTHF in the template crystal structure (Fig. 3). Also, one of the quinoxaline nitrogens forms a weak H bond with Asn484. This extensive H bonding network, together with the relatively rigid scaffold which is complementary to the MeTHF pocket, could rationalize the high potency of **5c** (Fig. 3). Interestingly, mapping of the electrostatic potential on the Connolly surface of **5c** and tetrahydrofolate reveals an obvious similarity (Fig. 4). Also, the distances between the groups responsible for the critical H bonding in both compounds are similar, 13.2 Å and 13.5 Å for **5c** and tetrahydrofolate, respectively (Fig. 4, black arrows).

Compound **3g** shares a comparable binding pattern with **5c**, particularly its benzimidazole nucleus. However, it forms only two H bonds with Asn458 and Asn 567. The unsubstituted benzamide moiety is not able to interact with Arg579 (Fig. 5). Finally, we tried to dock the uncompetitive inhibitor **3j** to understand its inability to bind to the MeTHF pocket. A distance constraint between the benzimidazole NH and Asn458 was applied to force the docking of this compound into the MeTHF binding site. This

Table 2
Chemical structures and IC_{50} of the quinoxaline series

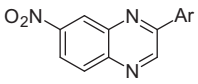

Compound	Ar	IC_{50} (μM)
5a		90
5b	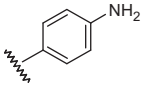	74
5c	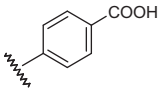	9
5d	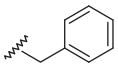	70
6a	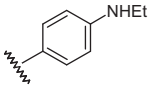	101
6b	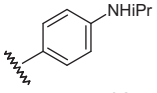	NA[a]
7a	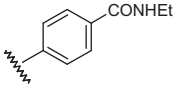	82
7b	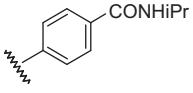	NA

Values were determined using highly purified rat liver methionine synthase.
[a] NA: not active.

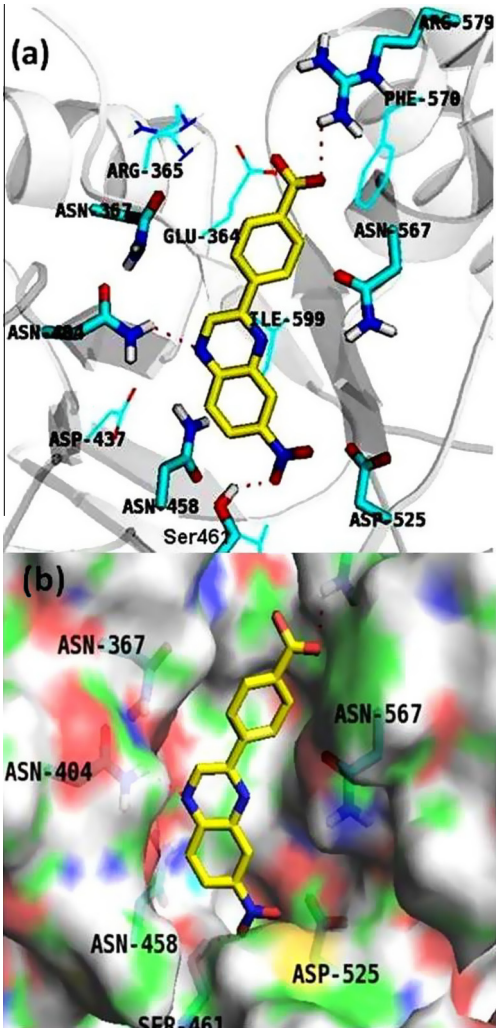

Figure 3. Proposed binding mode of **5c** in the homology model of rat MetS. (a) Cartoon representation with amino acid residue colored cyan and **5c** colored yellow. (b) Surface representation of the binding site with **5c** colored yellow. Shape complementarity between **5c** scaffold and the binding site is obvious.

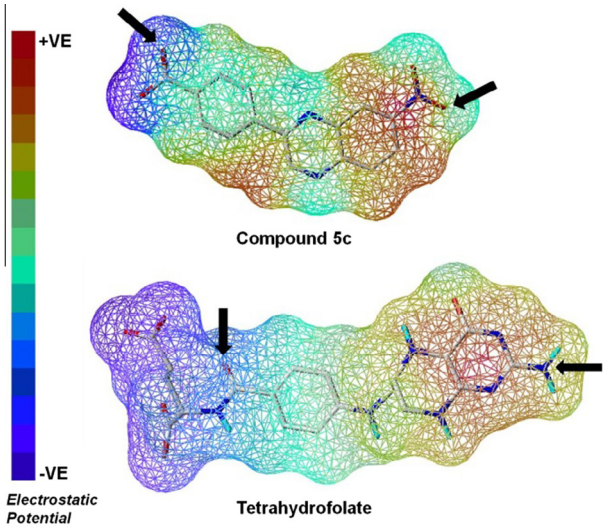

Figure 4. Mapping of the electrostatic potential on the Connolly surface of **5c** and tetrahydrofolate. Black arrows indicate the functional groups responsible for the critical H bonding with MetS.

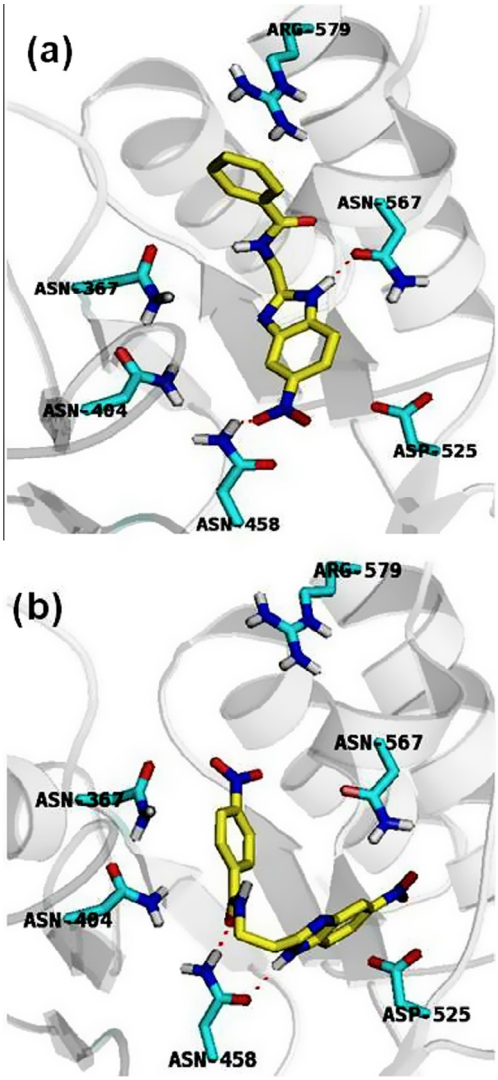

Figure 5. Proposed binding mode of (a) **3g** and (b) **3j** in the homology model of rat MetS. Cartoon representation is used with amino acid residues colored cyan and compounds colored yellow.

compound forms H bond with Asn458 only. In addition, the obvious internal strain in the docked conformation of **3j** was found to deteriorate its docking score. The bulky and relatively rigid nature of this compound did not allow the proper extended orientation in the MeTHF pocket adapted by **5c** (Fig. 5). These factors could provide, at least, a partial explanation of the inability of **3j** to compete with MeTHF for MetS binding.

3. Conclusion

MetS inhibitors represent a promising class of chemotherapeutic agents. Based on the scaffold of MeTHF and the previously reported inhibitors of the benzimidazole class, a novel series of benzimidazoles and quinoxalines were designed and tested in a cell-free assay for MetS inhibitory activity. Some of the prepared derivatives showed significant inhibition of the MetS reaction, especially relatively small quinoxalines and nitrobenzimidazoles. The most three active compounds, **5c**, **3g**, and **3j** were evaluated in a kinetic enzyme assay and, interestingly, the results indicated that there is more than one mode of interaction with the enzyme. Homology modeling and docking studies gave partial explanation for the differential binding of the prepared compounds to MeTHF. The ideal MetS competitive inhibitor should possess a benzo-fused nitrogen heterocycle, as a pteridine isostere, connected via a polar flexible linker to an aryl group which is able to occupy the PABA binding pocket. It is worth noting that compounds reported in this study represent the first class of non-folate MetS inhibitors targeting the PABA pocket. On the other hand, more detailed mechanistic and computational studies on a large number of compounds are required to unveil the molecular determinants of uncompetitive inhibition. This study revealed a new generation of lead compounds that could help in the design of clinically useful MetS inhibitors with potential anticancer activity.

4. Experimental

4.1. Chemistry

The structures of all tested compounds were confirmed by ^{1}H NMR, ^{13}C NMR and mass spectrometry (ESI). The purities of the tested compounds were determined by combustion analysis and are 95% or higher. Commercial chemicals and solvents were reagent grade and used without further purification. ^{1}H and ^{13}C NMR spectra were measured in DMSO-d_6 on a Bruker ARX 400. Chemical shifts are reported in parts per million (ppm) using tetramethylsilane (TMS) as an internal standard. Mass spectra were obtained on a Fissous Instruments VG Platform 2 (ESI-MS system). Combustion analysis was performed at the Microanalytical Center of Cairo University, Egypt. The synthetic procedure for the compounds is illustrated in Schemes 1 and 2.

4.1.1. General procedures for the synthesis of (1*H*-benzimidazole-2-yl)alkylamines (2a–d)

General procedure for the synthesis of (1*H*-benzimidazole-2-yl)alkylamines was adapted from the Phillips procedure.[18] L-Amino acid was added to a stirred solution of 4-nitro-*o*-phenylendiamine and aqueous HCl (5.5 M). The mixture was heated under reflux for 5 h. The blue reaction mixture was cooled to room temperature. The mixture was allowed to stand for overnight where upon the desired (1*H*-benzimidazole-2-yl)alkylamine was crystallized in its HCl salt form. The free base was obtained by neutralization of the reaction mixture with 1 M K_2CO_3 solution followed by extraction with ethyl acetate. The extract was evaporated to dryness and recrystallized from an ethanol.

4.1.2. 1-(1*H*-Benzimidazol-2-yl)methanamine (2a)

Yield 61%; mp 269–270 °C. ^{1}H NMR (400 MHz, DMSO-d_6): δ 7.61 (2H, dd, ^{3}J 9.40, ^{4}J 3.20, 4-H, 7-H), 7.27 (2H, m, ^{3}J 9.40, ^{4}J 3.20, 5-H, 6-H), 4.43 (2H, s, CH_2), 5.02 (3H, br, s, NH, NH_2,); ^{13}C NMR (400 MHz, DMSO-d_6): δ 147.56 (C-2), 132.51 (C-3a, C-7a), 126.16 (C-5, C-6), 114.99 (C-4, C-7), 35.17 (C-1′); DEPT (135) (DMSO-d_6); CH_2: 35.17, CH: 126.16, 114.99; IR (KBr): 3050 (C–H, sp^2), 2850 (C–H, sp^3), 1450 and 1350 (C–H, bend) cm^{-1}; MS (EI): *m*/*z* 147.19 (M^+). Anal. Calcd for $C_8H_9N_3$: C, 65.29; H, 6.16; N, 28.55. Found; C, 64.99; H, 6.36; N, 28.43.

4.1.3. 2-(1*H*-Benzimidazol-2-yl)ethanamine (2b)

Yield 66%; mp 269–270 °C. ^{1}H NMR (400 MHz, DMSO-d_6): δ 8.57 (2H, br, s, NH_2), 7.79 (2H, dd, ^{3}J 9.40, ^{4}J 3.21, 4-H, 7-H), 7.53 (2H, dd, ^{3}J 9.40, ^{4}J 3.21, 5-H, 6-H), 3.56 (4H, m, CH_2CH_2); ^{13}C NMR (400 MHz, DMSO-d_6): δ 150.8 (C-2), 131.6 (C-3a, C-7a), 126.1 (C-5, C-6), 114.3 (C-4, C-7), 36.3 (C-2′), 25.2 (C-1′); IR (KBr): 3500 (N–H), 3050 (C–H, sp^2), 2850 (C–H, sp^3), 1450 and 1350 (C–H, bend) cm^{-1}; MS (EI): *m*/*z* 161.17 (M^+). Anal. Calcd for C9H11N3: C, 67.06; H, 6.88; N, 26.07. Found; C, 67.35; H, 6.80; N, 26.77.

4.1.4. 1-(5-Nitro-1*H*-benzimidazol-2-yl)methanamine (2c)

Yield 40%; mp 248–251 °C. ^{1}H NMR (400 MHz, DMSO-d_6): δ 10.90 (1H, br, s, NH), 8.90 (2H, br, s, NH_2), 8.51 (1H, d, ^4J 1.97, 4-H), 8.15 (1H, dd, ^3J 8.90, ^4J 2.23, 6-H), 7.78 (1H, d, ^3J 8.90, 7-H), 4.41 (2H, s, CH_2); ^{13}C NMR (400 MHz, DMSO-d_6): δ 153.7 (C-2), 143.2 (C-7a), 142.5 (C-5), 138.0 (C-3a), 118.7 (C-6), 115.3 (C-7), 112.9 (C-4), 36.92 (CH_2NH_2); DEPT 135 (DMSO-d_6) CH_2: 36.92, CH: 118.7, 115.3, 112.9; IR (KBr): 3400 (N–H), 3050 (C–H, sp^2), 2850 (C–H, sp^3), 1500 and 1350 (N–O); MS (EI): *m*/*z* 192.08 (M^+); Anal. Calcd for $C_8H_8N_4O_2{\cdot}2HCl{\cdot}1/4H_2O$: C, 35.60; H, 3.89; N, 20.77. Found; C, 35.92; H, 3.80; N, 20.43.

4.1.5. 2-(5-Nitro-1*H*-benzimidazol-2-yl)ethanamine (2d)

Yield 58%; mp >300 °C (decomp.). ^{1}H NMR (400 MHz, DMSO-d_6): δ 11.74 (1H, br, s, NH), 8.53 (1H, d, 4-H), 8.29 (1H, dd, ^3J 6.2, 6-H), 7.89 (1H, d, ^3J 6.2, 7-H), 3.52 (4H, m, CH_2CH_2); NH_2 not observed; ^{13}C NMR (400 MHz, DMSO-d_6): δ 155.9 (C-2), 144.6 (C-7a), 137.7 (C-5), 133.5 (C-3a), 120.5 (C-6), 115.2 (C-7), 111.2 (C-4), 36.4 (C-2′), 26.1 (C-1′); IR (KBr): 3450 (N–H), 3050 (C–H, sp^2), 2850 (C–H, sp^3), 1500 and 1350 (N–O); MS (EI): *m*/*z* 206.22 (M^+); Anal. Calcd for $C_9H_{12}N_4O_2{\cdot}2HCl{\cdot}H_2O$: C, 36.53; H, 4.32; N, 18.77. Found: C, 36.38; H, 4.73; N, 18.86.

4.1.6. General procedures for the acylation of (1*H*-benzimidazole-2-yl)alkylamines

Starting amino compound (0.238 mmol) was dissolved in THF (25 mL) and triethylamine (10 drops) was added to the stirred solution. Acyl halide (0.149 mmol) was added dropwise to the stirred solution, which was then heated under reflux for 3 h. The reaction mixture was concentrated under reduced pressure. The residue was dissolved in EtOAc and washed with aq. K_2CO_3 solution followed by brine. The organic layer was then dried over Na_2SO_4, filtered, and concentrated in vacuo. The residue was purified by silica gel column chromatography eluting with 1–5 methanol/DCM v/v.

4.1.7. *N*-((1*H*-Benzimidazole-2-yl)methyl)acetamide (3a)

Pale brown powder; yield 85%; mp 196–197 °C. ^{1}H NMR (400 MHz, DMSO-d_6): δ 9.26 (1H, d, ^3J 5.44, NH), 7.45 (2H, dd, ^3J 9.40, ^4J 3.21, 4-H, 7-H), 7.11 (2H, dd, ^3J 9.15, ^4J 3.21, 5-H, 6-H), 4.47 (2H, d, ^3J 5.69, 1′-H), 1.89 (3H, s, CH_3); ^{13}C NMR (400 MHz, DMSO-d_6): δ 170.1 (C=O), 153.2 (C-2), 131.2 (C-3a, C-7a), 126.3 (C-5, C-6), 114.4 (C-4, C-7), 37.6 (C-1′), 23.1 (C–CH_3); MS (EI): *m*/*z* 189.15 (M^+). Anal. Calcd for $C_{10}H_{11}N_3O$: C, 63.48; H, 5.86; N, 22.21. Found; C, 63.55; H, 5.79; N, 21.70.

4.1.8. *N*-(2-(1*H*-Benzimidazole-2-yl)ethyl)acetamide (3b)

White powder; yield 80%; mp 186–187 °C. ^{1}H NMR (400 MHz, DMSO-d_6): δ 8.05 (1H, t, ^3J 5.40, NH), 7.47 (2H, dd, 4-H, 7-H), 7.11 (2H, dd, ^3J 9.10, ^4J 3.10, 5-H, 6-H), 3.36 (2H, t, ^3J 7.17, 2′-H), 2.49 (2H, m, 1′-H), 1.78 (3H, s, CH_3); ^{13}C NMR (400 MHz, DMSO-d_6): δ 169.85 (C-4′), 153.4 (C-2), 133.6 (C-3a, C-7a), 121.74 (C-5, C-6), 121.7 (C-4, C-7), 37.8 (C-2′), 29.5 (C-1′), 23.2 (CH_3). MS (EI): *m*/*z* 203.16 (M^+). Anal Calcd for: $C_{11}H_{13}N_3O$: C, 65.01; H, 6.45; N, 20.68. Found: C, 65.09; H, 6.65; N, 20.38.

4.1.9. *N*-((5-Nitro-1*H*-benzimidazole-2-yl)methyl)acetamide (3c)

Yellow powder; yield 72%; mp 214–216 °C. ^{1}H NMR (400 MHz, DMSO-d_6): δ 8.63 (1H, t, ^3J 5.93, CH_2NH), 8.40 (1H, d, ^4J 2.22, 4-H), 8.10 (1H, dd, ^3J 8.90, ^4J 2.22, 6-H), 7.67 (1H, d, ^3J 8.90, 7-H), 4.52 (2H, d, ^3J 5.69, CH_2), 3.34 (1H, br, s, NH), 1.93 (3H, s, CH_3); ^{13}C NMR (400 MHz, DMSO-d_6): δ 171.3 (C=O), 157.8 (C-2), 144.6 (C-5), 138.0 (C-7a), 133.9 (C-3a), 120.3 (C-6), 115.3 (C-7), 111.5 (C-4), 36.8 (C-1′), 22.9 (CH_3); DEPT (135) (DMSO-d_6); CH_3: 22.9; CH_2: 36.8; CH: 120.3; 115.3, 111.5; IR (KBr): 3050 (C–H, sp^2), 2850 (C–H, sp^3), 1580 (C=O),1550 and 1350 (N–O) cm^{-1}; MS (EI): *m*/*z* 234.11 (M^+); Anal. Calcd for $C_{10}H_{10}N_4O_3$: C, 51.28; H, 4.30; N, 23.92. Found; C, 51.41; H, 4.10; N, 23.70.

4.1.10. *N*-(2(5-Nitro-1*H*-benzimidazole-2-yl)ethyl)acetamide (3d)

Pale yellow powder; yield 42%; mp 208–209 °C. ^{1}H NMR (400 MHz, DMSO-d_6): δ 8.43 (1H, d, ^4J 2.20, 4-H), 8.10 (2H, dd, ^3J 8.90, ^4J 2.20, 6-H, NH), 7.76 (1H, d, ^3J 8.90, 7-H), 3.56 (2H, t, ^3J 6.68, 2′-H), 3.08 (2H, t, ^3J 6.68, 1′-H), 1.82 (3H, s, CH_3); ^{13}C NMR (400 MHz, DMSO-d_6): δ 170.7 (C=O′), 157.4 (C-2), 145.3 (C-7a), 133.2 (C-5), 131.3 (C-3a), 121.3 (C-6), 115.3 (C-7), 110.9 (C-4), 36.9 (C-2′), 28.2 (C-1′), 23.0 (CH_3); IR (KBr): 3222 (N–H), 3061 (C–H, sp^2), 2931 (C–H, sp^3), 1665 (C=O), 1500 and 1344 (N=O) cm^{-1}; MS (EI): *m*/*z* 248.19 (M^+); Anal. Calcd for $C_{11}H_{12}N_4O_3$: C, 53.22; H, 4.87; N, 22.57. Found; C, 53.33; H, 4.66; N, 22.26.

4.1.11. *N*-(1*H*-Benzimidazole-2-yl-methyl)benzamide (3e)

Long white needles; Yield 95%; mp 234–235 °C. ^{1}H NMR (400 MHz, DMSO-d_6): δ 12.35 (1H, br, s, NH), 9.19 (1H, t, ^3J 5.7, CH_2-NH), 7.95 (2H, d, ^3J 6.9, 5′-H, 9′-H), 7.56–7.47 (5H, m, 4-H, 7-H, 6′-H, 7′-H, 8′-H), 7.13 (2H, dd, ^3J 7.4, 5-H, 6-H), 4.69 (2H, d, ^3J 5.7, CH_2); ^{13}C NMR (400 MHz, DMSO-d_6): δ 167.06 (C=O), 152.94 (C-2), 142.94 (C-3a, C-7a), 134.50 (C-7′), 131.99 (C-4′), 128.86 (C-6′, C-7′), 128.03 (C-5′, C-9′), 122.32 (C-5, C-6), 118.89 (C-4, C-7), 38.36 (C-1′); IR (KBr): 3050 (C–H, sp^2), 2850 (C–H, sp^2), 1700 (C=O), 1450 and 1350 (C–H, bend) cm^{-1}; MS (EI) *m*/*z* 251.11 (M^+); Anal Calcd for $C_{15}H_{13}N_3O$: C, 71.70; H, 5.21; N, 16.72. Found: C, 71.02; H, 5.38; N, 16.57.

4.1.12. *N*-(2-(1*H*-Benzimidazole-2-yl)ethyl)benzamide (3f)

Fine white needles; Yield 76%; mp 308–310 °C. ^{1}H NMR (400 MHz, DMSO-d_6): δ 12.40 (1H, s, NH), 8.70 (1H, t, ^3J 5.20, NH), 7.83 (2H, dd, ^3J 8.40, ^4J. 6′-H, 10′-H), 7.52–7.42 (5H, m, 4-H, 7-H, 8′-H, 7′H, 9′-H), 7.11 (2H, dd, ^3J 9.10, ^4J 2.80, 5-H, 6-H), 3.73 (2H, q, ^3J, 7.15, 2′-H), 3.12 (2H, t, ^3J 7.15, 1′-H); ^{13}C NMR (400 MHz, DMSO-d_6): δ 167.3 (C=O), 152.7 (C-2), 134.4 (C-3a, C-7a), 131.9 (C-5′), 131.3 (C-8′), 128.8 (C-7′, C-9′), 127.8 (C-6′, C-10′) 126.1 (C-5, C-6), 114.2 (C-4, C-7), 37.6 (C-2′), 27.6 (C-1′); DEPT 135 (600 MHz; DMSO-d_6) CH_2: 38.6, 29.4; CH: 131.7, 128.8, 127.7, 121.8, 121.7; IR (KBr): 3300 (N–H), 3025 (C–H, sp^2), 2850 (C–H, sp^3), 1635 (C=O); 1550 (N–H bend) cm^{-1}; MS (EI) *m*/*z* 265.18 (M^+). Anal. Calcd for $C_{16}H_{15}N_3O$: C, 72.43; H, 5.70; N, 15.84. Found; C, 72.88; H, 5.55; N, 15.66.

4.1.13. *N*-((5-Nitro-1*H*-benzimidazole-2-yl)methyl)benzamide (3g)

Pale yellow crystals; yield 68%; mp 244–246 °C. ^{1}H NMR (400 MHz, DMSO-d_6): δ 9.29 (1H, t, ^3J 5.93, NH), 8.41 (1H, d, ^4J 2.22, 4-H), 8.10 (1H, dd, ^3J 8.90, ^4J 2.22, 6-H), 7.94 (2H, dd, ^3J 8.16, 5′-H, 9′-H), 7.67 (1H, d, ^3J 8.90, 7-H), 7.66–7.47 (3H, m, 6′-H, 7′-H, 8′-H), 4.77 (2H, d, ^3J 5.93, CH_2); ^{13}C NMR (400 MHz, DMSO-d_6): δ 167.9 (C=O), 157.3 (C-2), 145.3 (C-7a), 135.8 (C-5), 133.3 (C-3a), 132.5 (C-7′), 131.4 (C-4′), 128.9 (C-6′, C-8′), 128.3 (C-5′, C-9′), 121.4 (C-6), 115.5 (C-7), 111.2 (C-4), 37.0 (C-1′); DEPT (135) (600 MHz; DMSO-d_6) CH_2: 37.0, CH: 132.5, 128.9, 128.3, 121.4, 115.5, 111.2; IR (KBr): 3500 (N–H), 3050 (C–H, sp^2), 2850 (C–H, sp^3), 1625 (C=O, conj.) 1550 and 1350 (N=O); 1300 (C–N) cm^{-1}; MS (EI) *m*/*z* 296.20 (M^+); Anal Calcd for: $C_{15}H_{12}N_4O_3$: C, 60.81; H, 4.08; N, 18.91. Found: C, 61.32; H, 3.99; N, 18.88.

4.1.14. *N*-(2-(5-Nitro-1*H*-benzimidazole-2-yl)ethyl)benzamide (3h)

Yellow powder; yield 98%, mp 197–200 °C. ^{1}H NMR (400 MHz, DMSO-d_6): δ 8.69 (1H, s, NH), 8.40 (1H, d, ^4J 2.22, 4-H), 8.09 (1H, dd ^3J 8.90, ^4J 2.22, 6-H), 7.82 (2H, d, ^3J 7.90, 6′-H, 10′-H), 7.67

(1H, d, ^3J 8.90, 7-H), 7.55–7.42 (3H, m ^3J 7.70, 7′-H, 8′-H, 9′-H), 3.37 (2H, q, ^3J 6.70, 2′-H), 3.17 (2H, t, ^3J 6.93, 1′-H), 1-H not observed; ^{13}C NMR (400 MHz, DMSO-d_6): δ 167.4 (C=O), 157.5 (C-2), 145.3 (C-7a), 135.7 (C-5), 134.4 (C-3a), 131.9 (C-7′), 131.3 (C-5′), 128.8 (C-7′, C-9′), 127.8 (C-6′, C-10′), 121.3 (C-1), 115.3 (C-7), 110.8 (C-4), 37.6 (C-2′), 28.2 (C-1′); DEPT (135) (600 MHz; DMSO-d_6) CH_2: 37.6, 28,2; CH: 131.9, 128.8, 127.8, 121.3, 115.3, 110.8; IR (KBr): 3308 (N–H), 3098 (C–H, sp^2), 2850 (C–H, sp^3), 1641.17 (C=O), 1505 and 1338 (NO) cm^{-1}; MS (EI): *m*/*z* 310.21 (M$^+$); Anal. Calcd for $C_{16}H_{14}N_4O_3$: C, 61.93; H, 4.55; N, 18.06. Found; C, 62.30; H, 4.49; N, 17.80.

4.1.15. *N*-((1*H*-Benzimidazole-2-yl)methyl)4-nitrobenzamide (3i)

Pale yellow powder; yield 44%; mp 128–130 °C. ^{1}H NMR (400 MHz, DMSO-d_6): δ 8.20 (2H, dd, ^3J 8.16, ^4J 2.22, 6′-H, 8′H), 7.67 (2H, dd, ^3J 8.41, 4-H, 7-H), 7.50 (2H, dd, ^3J 8.41, 5-H, 6-H), 7.14 (5H, m, ArH), 3.92 (4H, s, 2CH_2), NHs not observed; ^{13}C NMR (400 MHz, DMSO-d_6): δ 154.01 (C-7′), 148.81 (C-4′), 147.32 (C-2), 147.02 (C-3a, C-7a), 130.31 (C-5′, C-9′), 129.71 (C-5, C-6), 123.85 (C-6′, C-8′), 121.92 (C-4, C-7), 52.02 (C-3′), 46.65 (C-1′); IR (KBr): 3400 (C–N), 3067 (C–H, sp^2), 2832 (C–H, sp^3), 1517 and 1344 (N–O) cm^{-1}; MS (EI): *m*/*z* 296.17 (M$^+$). Anal. Calcd for: $C_{15}H_{12}N_4O_3$: C, 60.81; H, 4.08; N, 18.91. Found: C, 80.18; H, 4.14; N, 19.20.

4.1.16. 4-Nitro-*N*-(2-(5-nitro-1*H*-benzimidazol-2-yl)ethyl)benzamide (3j)

Yellow powder; yield 36%; mp 198–200 °C. ^{1}H NMR (400 MHz, DMSO-d_6): δ 8.43 (1H, d, ^4J 2.22, 4-H), 8.35 (2H, d, ^3J 8.65, 7′-H, 9′-H), 8.10 (1H, dd, ^3J 8.90, ^4J 2.22, 6-H), 7.90 (2H, d, ^3J 8.65, 6′-H, 10′-H), 7.70 (1H, d, ^3J 8.90, 7-H), 4.42 (2H, s, 4′-H, CH_2), 3.44 (4H, m, ^3J 5.93, 1′-H, 2′-H). ^{13}C NMR (400 MHz, DMSO-d_6): δ 155.4 (C-2), 148.2 (C-8′), 145.6 (C-7a), 138.8 (C-5), 138.2 (C-5′), 136.2 (C-3a), 132.0 (C-6′, C-10′), 124.1 (C-7′, C-9′), 120.9 (C-6), 115.3 (C-7), 111.1 (C-4), 49.5 (C-4′), 43.7 (C-2′), 38.9 (C-1′); DEPT (135) (DMSO-d_6) CH_2: 49.5, 43.7, 38.9; CH: 132.0, 124.1, 120.9 115.3; 111.1; MS (EI): *m*/*z* 355.11 (M$^+$). Anal. Calcd for $C_{16}H_{13}N_5O_5$: C, 54.09; H, 3.69; N, 19.71. Found; C, 53.59; H, 3.77; N, 19.66.

4.1.17. General procedure for the synthesis of 4-nitro-*N*-arylidene-1,2-phenylenediamine

4-Nitro-*o*-phenylendiamine **1** (2.69, 17.6 mmol) was suspended in 10 ml dry ethanol. The appropriate aldehyde (20.6 mmol) was dissolved in another 10 ml of dry ethanol and added to the above suspension. The mixture was heated under reflux for 12 h. The reaction was cooled on an ice bath and the precipitate was collected by filtration and washed with ethanol.

4.1.18. 4-Nitro-*N*-benzylidene-1,2-phenylenediamine (4a)

Brown crystalline solid; yield 84%; mp 120 °C. ^{1}H NMR (400 MHz, DMSO-d_6): δ 7.91 (1H, dd, ^3J 4.40, ^4J 3.20, 5-H), 7.87 (1H, s, 3-H), 7.77 (1H, d, ^3J 9.40, 6-H), 6.65 (5H, m, ArH), 5.69 (1H, s, 7-H), 5.40 (2H, brs, NH_2); IR (KBr): 3200 (NH_2), 3050 (C–H, sp^2), 1450 and 1350 (C–H, bend) cm^{-1}; MS (EI): *m*/*z* 241.09 (M$^+$). Anal. Calcd for: $C_{13}H_{11}N_3O_2$: C, 64.72; H, 4.60; N, 17.42. Found: C, 64.28; H, 4.19; N, 17.20.

4.1.19. 4-Nitro-*N*-(4-aminobenzylidene)-1,2-phenylenediamine (4b)

Green crystalline solid; 64%; mp 210 °C. ^{1}H NMR (400 MHz, DMSO-d_6): δ 8.32 (2H, br s, NH_2), 8.01 (1H, d, ^3J 2.10, 5-H), 7.97 (1H, s, 3-H), 7.72 (1H, d, ^3J 2.10, 6-H), 6.65–6.22 (5H, m, ArH), 5.99 (1H, s, 7-H), IR (KBr): 3200 (NH_2), 3050 (C–H, sp^2), 1450 and 1350 (NO_2, asymmetric bending) cm^{-1}; MS (EI): *m*/*z* 256.20 (M$^+$). Anal. Calcd for: $C_{13}H_{12}N_4O_2$: C, 60.93; H, 4.72; N, 21.86. Found: C, 60.83; H, 4.70; N, 22.08.

4.1.20. 4-(((2-Amino-5-nitrophenyl)imino)methyl)benzoic acid (4c)

Brown crystalline solid; 77%; mp 270 °C. ^{1}H NMR (400 MHz, DMSO-d_6): δ 9.12 (1H, br s, OH), 8.31 (1H, d, ^3J 1.20, 5-H), 7.87 (1H, d, ^4J 3.20, 3-H), 7.77 (1H, d, ^3J 9.40, 6-H), 6.65 (4H, m, ArH), 5.69 (1H, s, 7-H), 5.40 (2H, br s, NH_2); IR (KBr): 3400 (OH), 3170 (NH_2), 3050 (C–H, sp^2), 1450 and 1350 (C–H, bend), 1660 (C=O), 1390 (NO_2) cm^{-1}; MS (EI): *m*/*z* 285.09 (M$^+$). Anal. Calcd for: $C_{14}H_{11}N_3O_4$: C, 58.95; H, 3.89; N, 14.73. Found: C, 59.33; H, 4.01; N, 14.50.

4.1.21. 4-Nitro-*N*-(phenylethylidene)-1,2-phenylenediamine (4d)

Yellow solid; yield 41%; mp 199 °C. ^{1}H NMR (400 MHz, DMSO-d_6): δ 8.55 (2H, br s, NH_2), 8.40 (1H, d, ^3J 3.12, 5-H), 8.07 (1H, s, ^4J 1.20, 3-H), 8.02 (1H, d, ^3J 3.12, 6-H), 7.88 (5 H, m, ArH), 6.01 (1H, t, ^3J 2.22, 7-H), 2.20 (2H, d, ^3J 2.12, CH_2); MS (EI): *m*/*z* 255.19 (M$^+$). Anal. Calcd for: $C_{14}H_{13}N_3O_2$: C, 65.87; H, 5.13; N, 16.46. Found: C, 65.58; H, 4.74; N, 16.21.

4.1.22. General procedures for the synthesis of 7-nitro-2-arylquinoxaline (5a–d)

4-Nitro-*N*-arylidene-1,2-phenylenediamine **4a–d** (8.5 mmol) was dissolved in 15 ml DMF at room temperature and triethyl orthoformate (6.36 mL, 43 mmol) was added. The mixture was heated under reflux for 24 h and subsequently allowed to cool to room temperature and evaporated to dryness. The residue was purified using column chromatography eluting with toluene/ethyl acetate 2:1.

4.1.23. 7-Nitro-2-phenylquinoxaline (5a)

Yellow crystalline solid; yield 74%; mp 210 °C. ^{1}H NMR (400 MHz, DMSO-d_6): δ 8.90–6.46 (9H, m, ArH); IR (KBr): 3020 (C–H, sp^2), 1630 (C=C, sp^2), 1440 (C=N), 1330 (NO_2) cm^{-1}; MS (EI): *m*/*z* 251.15 (M$^+$); Anal Calcd for $C_{14}H_9N_3O_2$: C, 66.93; H, 3.61; N, 16.73. Found: C, 67.04; H, 4.01; N, 16.22.

4.1.24. 4-(7-Nitroquinoxalin-2-yl)aniline (5b)

Brown crystalline solid; 47%; mp 222 °C. ^{1}H NMR (400 MHz, DMSO-d_6): δ 9.22 (2H, br s, NH_2), 8.90–6.05 (8H, m, ArH); IR (KBr): 3400 (forked NH_2), 3100 (C–H, sp^2), 1699 (C=C, sp^2), 1546 (C=N), 1300 (NO_2) cm^{-1}; MS (EI): *m*/*z* 266.17 (M$^+$); Anal. Calcd for $C_{14}H_{10}N_4O_2$: C, 63.15; H, 3.79; N, 21.04. Found: C, 63.07; H, 4.11; N, 21.40.

4.1.25. 4-(7-Nitroquinoxalin-2-yl)benzoic acid (5c)

Pale yellow solid, yield 25; mp 310 °C. ^{1}H NMR (400 MHz, DMSO-d_6): δ 9.52 (1H, br s, OH), 7.99–6.25 (8H, m, ArH); IR (KBr): 3550 (OH), 3206 (C–H, sp^2), 1600 (C=C, sp^2), 1396 (NO_2) cm^{-1}; MS (EI): *m*/*z* 295.10 (M$^+$); Anal. Calcd for $C_{15}H_9N_3O_4$: C, 61.02; H, 3.07; N, 14.23. Found: C, 61.37; H, 3.51; N; 14.06.

4.1.26. 2-Benzyl-7-nitroquinoxaline (5d)

Brown crystalline solid; yield; 47%; mp 280 °C. ^{1}H NMR (400 MHz, DMSO-d_6): δ 9.50–6.05 (9 H, m, ArH), 2.99 (2H, s, CH_2); IR (KBr): 1590 (C=C, sp^2), 1309 (NO_2) cm^{-1}; MS (EI): *m*/*z* 266.17 (M$^+$); Anal. Calcd for $C_{15}H_{11}N_3O_2$: C, 67.92; H, 4.18; N, 15.84. Found: C, 67.07; H, 4.51; N; 15.26.

4.1.27. General procedure for the synthesis of *N*-alkyl-4-(7-nitroquinoxalin-2-yl)aniline (6a–b)

4-(7-Nitroquinoxalin-2-yl)aniline (**5b**) (0.12 g, 0.476 mmol) was dissolved in 25 ml THF and, then, triethylamine (10 drops) was added to the stirred solution. Alkyl bromide (0.149 mmol) was added dropwise to the mixture, which was then heated under reflux for 24 h. The reaction mixture was concentrated under

reduced pressure. The crude product was dissolved in dichloromethane and washed with water (3 × 10 mL). The organic layer was dried over $MgSO_4$, filtered and concentrated under reduced pressure to yield a yellow precipitate, which was purified with column chromatography eluting with DCM/ethylacetate 2:5.

4.1.28. *N*-Ethyl-4-(7-nitroquinoxalin-2-yl)aniline (6a)

Bright yellow crystals; yield 75%; mp 213–216 °C. ^{1}H NMR (400 MHz, DMSO-d_6): δ 8.94 (1H, s, NH), 8.50–6.50 (13H, m, ArH), 3.99 (2H, q, ^3J 2.1, CH_2), 1.33 (3H, t, ^3J 2.1, CH_3); MS (EI) *m*/*z* 294.21 (M^+); Anal. Calcd for $C_{16}H_{14}N_4O_2$: C, 65.30; H, 4.79; N, 19.04. Found: C, 65.00; H, 5.09; N; 18.86.

4.1.29. *N*-Isopropyl-4-(7-nitroquinoxalin-2-yl)aniline (6b)

Yellow solid; yield 25%; mp 262–265 °C. ^{1}H NMR (400 MHz, DMSO-d_6): δ 8.99–6.50 (8H, m, ArH), 4.94 (1H, s, NH), 2.99–1.01 (11H, m, $CH_{aliphatic}$); MS (EI) *m*/*z* 308.15 (M^+); Anal. Calcd for $C_{17}H_{16}N_4O_2$: C, 66.22; H, 5.23; N, 18.17. Found: C, 65.90; H, 5.29; N; 17.79.

4.1.30. General procedure for the synthesis of *N*-alkyl-4-(7-nitroquinoxalin-2-yl)benzamide (7a–b)

To a solution of amine HCl (0.3 mmol) in CH_2Cl_2 (5 ml) were added 4-(7-nitroquinoxalin-2-yl)benzoic acid (**5c**) (106 mg, 0.36 mmol), HOBt (42 mg, 0.36 mmol), EDCI (90 mg, 0.45 mmol) and Et_3N (0.21 mL, 1.5 mmol), and this mixture was stirred at room temperature for 12 h. The mixture was then partitioned between CH_2Cl_2 and saturated $NaHCO_3$ aqueous solution and the organic layer was washed with brine, dried over Na_2SO_4, filtered, and concentrated in vacuo. The crude residue was purified by silica gel column chromatography $CHCl_3$/MeOH (96:4) to yield the required amide.

4.1.31. *N*-Ethyl-4-(7-nitroquinoxalin-2-yl)benzamide (7a)

Bright yellow needles; yield 27%; mp 274–276 °C. ^{1}H NMR (400 MHz, DMSO-d_6): δ 9.44 (1H, s, NH), 9.22 (1H, s, OH), 8.93–6.91 (8H, m, ArH), 3.01 (2H, q, ^3J 4.1, CH_2), 2.63 (3H, t, ^3J 4.66, CH_3); IR (KBr): 3600 (amide N–H stretching), 3166 (C–H, sp^2), 1690 (amide C=O stretching), 1600 (C=C, sp^2), 1396 (NO_2) cm^{-1}; MS (EI) *m*/*z* 322.19 (M^+); Anal. Calcd for $C_{17}H_{14}N_4O_3$: C, 63.35; H, 4.38; N, 17.38. Found: C, 63.90; H, 4.99; N; 17.06.

4.1.32. *N*-Isopropyl-4-(7-nitroquinoxalin-2-yl)benzamide (7b)

Bright yellow solid; yield 24%; mp 200–202 °C. ^{1}H NMR (400 MHz, DMSO-d_6): δ 9.20 (1H, s, NH), 8.81–7.01 (8H, m, ArH), 4.01 (1H, m, CH), 3.99 (4H, m, CH_2), 1.33 (6H, m, CH_3); MS (EI) *m*/*z* 336.21 (M^+); Anal. Calcd for $C_{18}H_{16}N_4O_3$: C, 64.28; H, 4.79; N, 16.66. Found: C, 64.90; H, 5.00; N; 16.06.

4.2. Biological evaluation

4.2.1. Enzyme purification

Methionine synthase was isolated and purified from rat liver according to the reported procedure.[24,25] Rat liver homogenate was prepared in the presence of a cocktail of protease inhibitors. The cytosolic fraction was obtained following a series of centrifugation steps. This preparation was initially purified using batch chromatography on DEAE cellulose. The speedy removal of unwanted proteins in the unbound fraction enriched the enzyme preparation and facilitated the next step of the purification which was performed using column chromatography. Anion exchange chromatography using DEAE and Q-sepharose resins was used to purify MetS through electrostatic attractions. Bound proteins were eluted by increasing the ionic strength of the buffer to 500 mm NaCl. The bound proteins were eluted at 2 mL/min and fractions were collected at selected intervals throughout the run. Fraction collection commenced at the beginning of each peak until it tailed off. The active fractions were pooled, desalted, and concentrated using an Amicon ultrafiltrator fitted with a 30 kDa membrane. Further purification of the enzyme was performed using a hydroxyapatite column eluting with potassium phosphate buffer (gradient: 20–500 mM). The active fractions of MetS were collected, deionized and concentrated by ultrafiltration. The final enzyme preparation was stored at 20 °C, out of direct light.

4.2.2. Methionine synthase assay

MetS activity was determined according to the procedure reported by Kenyon et al.[26] Reactions contained 50 mM phosphate buffer (pH 7.4), 227 μM ^{14}C-5-methyltetrahydrofolate, 23 mM dithiothreitol, 40 μM *S*-AdoMet, 60 μM hydroxycobalamin, the enzyme source, and DMSO solution of the inhibitor (5 μM). The reaction mixture was incubated in light-excluding sealed serum vials under N_2 gas. After pre-incubation for 5 min, the reaction was initiated by the addition of 500 μM homocysteine and incubated at 37 °C for 30 min. The reaction was terminated by the addition of ice-cold water (400 μM). The reaction mixture was passed through a 0.5 × 5 cm AG1-X8 resin column. [^{14}C] Methionine was eluted with 2 mL of water and quantified using a liquid scintillation counter (Packard Tricarb 1900CA; Perkin Elmer).

4.2.3. Determination of K_m and V_{max} for 5-methyltetrahydrofolate

In all the three assays, a constant concentration of Hcy (500 μM) was used. Assays were incubated for 10 min at varying concentrations of 5-methyltetrahydrofolate (0, 50, 100, 500 and 1000 μM). Initially, the incubation time and the enzyme concentration were altered in order to establish conditions for linear kinetics. Then, the protein concentration was adjusted to ensure that the initial velocities were correctly estimated.

4.3. Homology modeling

Multiple sequences of three MetS enzymes were used in the alignment process. Sequences of human, rat, *Thermotoga maritima* MetS were aligned using the web interface ClustalW (Fig. S2).[27] The multiple sequence alignment obtained in the previous step was used together with the crystal structure of *Thermotoga maritima* MetS (PDB: 1Q8J) as an input for the building of the homology model of the rat MetS using MODELLER 9v3 software.[28] After all the hydrogens were added, the crude model was minimized in a stepwise manner using OPLS-2005 force field[29] in Macromodel v8.0 (Schrodinger Inc., Portland, OR, USA) in order to relieve any steric clashes or distorted geometries. Five steps of minimization were carried out. In the first step, all heavy atoms were kept fixed (force constant: 500 kcal/mol/Å^2) and only water and hydrogens were allowed to minimize and relax their positions. During the second step protein side chains were kept flexible while keeping the protein backbone restrained with the same force constant. The last three steps involved minimization of the whole protein with gradually reducing force constraints of 50, 25, and 10 kcal/mol/Å^2 on the C_α atoms of the backbone. The five minimization steps consisted of 6000 steps each, in which the first 1000 steps were steepest descents, and the last 5000 were conjugate gradient.[30]

4.4. Docking

Compounds **5c**, **3g**, and **3j** were built and energy-minimized using MMFF charges and the MMFF force field as implemented in Sybyl X.1 with 2000 steps of the conjugate gradient method to a gradient of 0.001 kcal/Å.[31] CCDC GOLD 4.12 software was used for docking of the minimized compounds into the putative binding

pocket of the developed homology model of rat MetS.[32] This software uses a genetic algorithm (GA) to explore possible ligand binding modes by changing dihedrals of ligand rotatable bonds, ligand ring geometries, and dihedrals of protein OH and NH_2 groups. The binding site was defined to include all amino acid residues within 10 Å of the side chain nitrogen of Asn458 with no distance restraints unless otherwise indicated. Docking was carried out using the standard mode settings and GoldScore, a molecular mechanics-like function depending on protein–ligand hydrogen bonding, protein–ligand van der Waals score, ligand intramolecular hydrogen bonding and ligand intramolecular strain.[33] A total of 10 genetic algorithm runs were performed for each ligand with early termination criteria set to 1.5 Å root-mean-square deviation (RMSD) value.

A. Supplementary data

Supplementary data associated with this article can be found, in the online version, at http://dx.doi.org/10.1016/j.bmc.2013.10.052.

References and notes

1. Drennan, C. L.; Huang, S.; Drummond, J. T.; Matthews, R. G.; Lidwig, M. L. *Science* **1994**, *266*, 1669.
2. Grabowski, M.; Banasiuk, R.; Wegrzyn, A.; Kedzierska, B.; Lica, J.; Banecka-Majkutewicz, Z.; Banecki, B. *Acta Biochim. Pol.* **2012**, *59*, 489.
3. Liu, Z. Z.; Zhang, J. T.; Liu, D.; Hao, Y. H.; Chang, B. M.; Xie, J.; Li, P. Z. *Chin. Med. J. (Engl)* **2013**, *126*, 865.
4. McCusker, K. P.; Medzihradszky, K. F.; Shiver, A. L.; Nichols, R. J.; Yan, F.; Maltby, D. A.; Gross, C. A.; Fujimori, D. G. *J. Am. Chem. Soc.* **2012**, *134*, 18074.
5. Wolthers, K. R.; Toogood, H. S.; Jowitt, T. A.; Marshall, K. R.; Leys, D.; Scrutton, N. S. *FEBS J.* **2007**, *274*, 738.
6. Evans, J. C.; Huddler, D. P.; Hilgers, M. T.; Romanchuk, G.; Matthews, R. G.; Ludwig, M. L. *Proc. Natl. Acad. Sci. U.S.A.* **2004**, *101*, 3729.
7. Partearroyo, T.; Perez-Miguelsanz, J.; Ubeda, N.; Valencia-Benitez, M.; Alonso-Aperte, E.; Varela-Moreiras, G. *Eur. J. Nutr.* **2013**, *52*, 1157.
8. Navarro-Martinez, M. D.; Cabezas-Herrera, J.; Rodriguez-Lopez, J. N. *Int. J. Antimicrob. Agents* **2006**, *28*, 560.
9. Wolthers, K. R.; Lou, X.; Toogood, H. S.; Leys, D.; Scrutton, N. S. *Biochemistry* **2007**, *46*, 11833.
10. Zhou, D.; Mei, Q.; Luo, H.; Tang, B.; Yu, P. *Int. J. Biol. Sci.* **2012**, *8*, 819.
11. Zhong, S.; Xu, J.; Li, W.; Chen, Z.; Ma, T.; Zhao, J. *Gene* **2013**, *531*, 8.
12. Waly, M. I.; Kharbanda, K. K.; Deth, R. C. *Alcohol Clin. Exp. Res.* **2011**, *35*, 277.
13. Culley, D. J.; Raghavan, S. V.; Waly, M.; Baxter, M. G.; Yukhananov, R.; Deth, R. C.; Crosby, G. *Anesth. Analg.* **2007**, *105*, 83.
14. Kenyon, S. H.; Alves, M.; Neubert, H.; Nicolaou, A.; Del Olmo, E.; Gibbons, W. A. *Biochem. Soc. Trans.* **1996**, *24*, 265S.
15. Brennt, C. E.; Smith, J. R. *Gen. Pharmacol.* **1989**, *20*, 427.
16. Zhang, Z.; Tian, C.; Zhou, S.; Wang, W.; Guo, Y.; Xia, J.; Liu, Z.; Wang, B.; Wang, X.; Golding, B. T.; Griff, R. J.; Du, Y.; Liu, J. *Eur. J. Med. Chem.* **2012**, *58*, 228.
17. Banks, E. C.; Doughty, S. W.; Toms, S. M.; Wheelhouse, R. T.; Nicolaou, A. *FEBS J.* **2007**, *274*, 287.
18. Dubey, R.; Hari Narayana Moorthy, N. S. *Chem. Pharm. Bull. (Tokyo)* **2007**, *55*, 115.
19. Ingle, R.; Marathe, R.; Magar, D.; Patel, H. M.; Surana, S. J. *Eur. J. Med. Chem.* **2013**, *65*, 168.
20. Prins, L. H.; Petzer, J. P.; Malan, S. F. *Bioorg. Med. Chem.* **2009**, *17*, 7523.
21. Poirson-Bichat, F.; Gonfalone, G.; Bras-Goncalves, R. A.; Dutrillaux, B.; Poupon, M. F. *Br. J. Cancer.* **1997**, *75*, 1605.
22. Bach, T. J.; Lichtenthaler, H. K. *Biochim. Biophys. Acta* **1984**, *794*, 152.
23. Hendrich, B.; Bird, A. *Curr. Top. Microbiol. Immunol.* **2000**, *249*, 55.
24. Waly, M.; Olteanu, H.; Banerjee, R.; Choi, S. W.; Mason, J. B.; Parker, B. S.; Sukumar, S.; Shim, S.; Sharma, A.; Benzecry, J. M.; Power-Charnitsky, V. A.; Deth, R. C. *Mol. Psychiatry* **2004**, *9*, 358.
25. Nicolaou, A.; Kenyon, S. H.; Gibbons, J. M.; Ast, T.; Gibbons, W. A. *Eur. J. Clin. Invest.* **1996**, *26*, 167.
26. Kenyon, S. H.; Waterfield, C. J.; Timbrell, J. A.; Nicolaou, A. *Biochem. Pharmacol.* **2002**, *63*, 381.
27. Clustalw2. http://www.ebi.ac.uk/Tools/clustalw2/index.html (accessed April 28.
28. Sali, A.; Blundell, T. L. *J. Mol. Biol.* **1993**, *234*, 779.
29. Kahn, K.; Bruice, T. C. *J. Comput. Chem.* **2002**, *23*, 977.
30. Gibon, D.; Rousseau, J.; Castelain, B.; Blond, S.; Vasseur, C.; Marchandise, X. *Int. J. Radiat. Oncol. Biol. Phys.* **1995**, *33*, 201.
31. Cheng, A.; Best, S. A.; Merz, K. M., Jr.; Reynolds, C. H. *J. Mol. Graph. Model.* **2000**, *18*, 273.
32. Jones, G.; Willett, P.; Glen, R. C.; Leach, A. R.; Taylor, R. *J. Mol. Biol.* **1997**, *267*, 727.
33. Annamala, M. K.; Inampudi, K. K.; Guruprasad, L. *Bioinformation* **2007**, *1*, 339.